

limited proliferative capacity (3). Recently, we have obtained more evidence (15) for the dominance of the senescence inhibitor in that microinjection of human c-H-ras DNA does not stimulate the entry of senescent cells into S phase. The c-H-ras DNA, when microinjected together with DNA coding for the E1A gene of adenovirus, is also unable to stimulate DNA synthesis in senescent cells. This combination of oncogene DNA's permits primary rodent cells to proceed to full transformation and tumorigenicity (16). These results support the observations of Sager *et al.* (17) that oncogene DNA, transfected into normal human cells, failed to endow them with tumorigenic potential. Sager (18) has proposed the existence of anti-oncogenes in normal cells that suppress the action of the oncogene protein products. We consider the senescent cell inhibitor gene a prime candidate for an anti-oncogene.

#### REFERENCES AND NOTES

1. L. Hayflick and P. S. Moorhead, *Exp. Cell Res.* **25**, 585 (1961).
2. L. Hayflick, *ibid.* **37**, 614 (1965).
3. O. M. Pereira-Smith and J. R. Smith, *Science* **221**, 964 (1983).
4. G. C. Burmer, C. J. Zeigler, T. H. Norwood, *J. Cell Biol.* **94**, 187 (1982).
5. C. K. Drescher-Lincoln and J. R. Smith, *Exp. Cell Res.* **153**, 208 (1984).
6. O. M. Pereira-Smith, S. F. Fisher, J. R. Smith, *ibid.* **160**, 297 (1985).
7. R. T. Dell'Orco, *Fed. Proc. Fed. Am. Soc. Exp. Biol.* **33**, 1969 (1974).
8. C. K. Lumpkin, Jr., J. K. McClung, J. R. Smith, *Exp. Cell Res.* **160**, 544 (1985); B. B. Kaplan, S. L. Bernstein, A. E. Gioio, *Biochem. J.* **183**, 181 (1979); O. M. Pereira-Smith and J. R. Smith, *Somatic Cell Genet.* **8**, 731 (1982).
9. M. R. Cappechi, *Cell* **22**, 479 (1980).
10. M. Yamaizumi, A. L. Horwich, F. H. Ruddle, *Mol. Cell. Biol.* **3**, 511 (1983).
11. T. Maniatis, E. F. Fritsch, J. Sambrook, *Molecular Cloning: A Laboratory Manual* (Cold Spring Harbor Laboratory, Cold Spring Harbor, NY, 1982).
12. G. C. Burmer, P. S. Rabinovitch, T. H. Norwood, *J. Cell. Physiol.* **118**, 97 (1984).
13. B. H. Cochran, A. C. Reffel, C. D. Stiles, *Cell* **33**, 939 (1983).
14. T. H. Norwood, W. R. Pendergrass, C. A. Sprague, G. M. Martin, *Proc. Natl. Acad. Sci. U.S.A.* **71**, 2231 (1974); R. M. Yanishevsky and G. H. Stein, *Exp. Cell Res.* **126**, 469 (1980); G. H. Stein and R. M. Yanishevsky, *ibid.* **120**, 155 (1979); L. Gordon, M. Beeson, *Proc. Natl. Acad. Sci. U.S.A.* **79**, 5287 (1982).
15. C. K. Lumpkin *et al.*, in preparation.
16. H. Land *et al.*, *Nature (London)* **304**, 596 (1983); H. E. Ruley, *ibid.*, p. 602; R. F. Newbold and R. W. Overell, *ibid.*, p. 648.
17. R. Sager *et al.*, *Proc. Natl. Acad. Sci. U.S.A.* **80**, 7601 (1983).
18. R. W. Craig and R. Sager, *ibid.* **82**, 2062 (1985).
19. It was possible that the high abundance inhibitor poly(A)<sup>+</sup> RNA found in senescent cells was simply a result of the presence of cells that are nonproliferating in high levels of serum growth factors (10 percent FBS). We tested this possibility by microinjecting poly(A)<sup>+</sup> RNA obtained from young cells that had been maintained in density-inhibited confluent culture (in medium containing 10 percent FBS) for 2 weeks after confluence was reached. When microinjected at a concentration of 1 mg/ml, about 20 percent inhibition was observed. Dilution to 0.1 mg/ml resulted in essentially no inhibition. Therefore, it seems that the high abundance of inhibitor RNA found in senescent cells is a property of *in vitro* cellular senescence rather than a non-age-related effect of serum concentration.
20. This work was supported by NIH grants AG-04749, AG-05333, and T32-CA-09197.

3 September 1985; accepted 21 February 1986

## Androgens Regulate the Dendritic Length of Mammalian Motoneurons in Adulthood

ELIZABETH M. KURZ,\* DALE R. SENGELAUB, ARTHUR P. ARNOLD

Sex steroid hormones have been thought to alter behaviors in adulthood by changing the activity of neural circuits rather than by inducing major structural changes in these pathways. In a group of androgen-sensitive motoneurons that mediate male copulatory functions, decreases in androgen levels after castration of adult rats produced dramatic structural changes, decreasing both the dendritic length and soma size of these motoneurons. These changes were reversed by androgen replacement. These results imply a surprising degree of synaptic plasticity in adult motoneurons and suggest that normal changes in androgen levels in adulthood are associated with significant alterations in the structure and function of these neurons.

**D**URING DEVELOPMENT, STEROID hormones produce permanent sexual dimorphisms in neuron number, morphology, and connectivity; in adulthood these neurons respond transiently to steroid hormones to produce sex-specific behaviors (1). In contrast to these dramatic developmental effects, steroid influences on neurons in adulthood are thought to be modest and impermanent (2). Until recently the actions of steroids in the adult were not thought to involve major structural changes, such as synaptic reorganization of steroid-sensitive neural circuits. However, such major alterations have been demonstrated in the avian brain; treatment of adult female canaries with androgens induces song behavior and stimulates dendritic growth and the formation of new synapses in at least one sexually dimorphic brain area involved in song (3). We now report that in a sexually dimorphic nucleus in the mammalian spinal

cord, the dendritic length of motoneurons is dramatically affected by variations in androgen levels during adulthood. The reversibility of this androgenic effect on dendritic length indicates a remarkable androgen-regulated structural plasticity. The neurons involved are important for copulatory behaviors (4), which are sensitive to alterations in androgen levels (5). Our results therefore suggest that the reversible effects of androgen on sexual behavior in adulthood are mediated in part by alterations in dendritic morphology and, consequently, in the synaptic organization of specific neural pathways.

The spinal nucleus of the bulbocavernosus (SNB) is a cluster of motoneurons located in the fifth and sixth lumbar segments of the rat spinal cord, and consists of approximately 200 motoneurons in adult males but only 60 in adult females. In males, the majority of SNB motoneurons innervate the muscles

bulbocavernosus (BC) and levator ani (LA) (6), which attach exclusively to the penis. In contrast, adult females lack the BC and LA musculature (7); their SNB motoneurons innervate the apparently nondimorphic anal sphincter, as do the remaining SNB motoneurons in males (8). Female SNB motoneurons are approximately 50 percent smaller than those of males (9). These sex differences in SNB motoneuron number, size, and projections, and differences in the presence of the SNB target musculature, are determined by the action of androgens during a critical perinatal period (7, 10). In adulthood, both the SNB motoneurons and their perineal target muscles accumulate androgens (11) and continue to be sensitive to androgenic effects. For example, after castration both SNB soma size and peripheral muscle mass are significantly reduced, but can be maintained at normal values by treatment with testosterone propionate (9, 12).

In our study we examined the length and distribution of the dendritic arbor of SNB motoneurons to determine if these aspects of dendritic morphology were also sensitive to androgen levels. Twenty-five adult male rats (Sprague-Dawley, Simonsen) were assigned to one of the following six groups: normal males 60 days old ( $n = 4$ ); males that were either castrated ( $n = 5$ ) or sham-

Department of Psychology and Laboratory of Neuroendocrinology, Brain Research Institute, University of California at Los Angeles, Los Angeles, CA 90024.

\*To whom correspondence should be addressed.

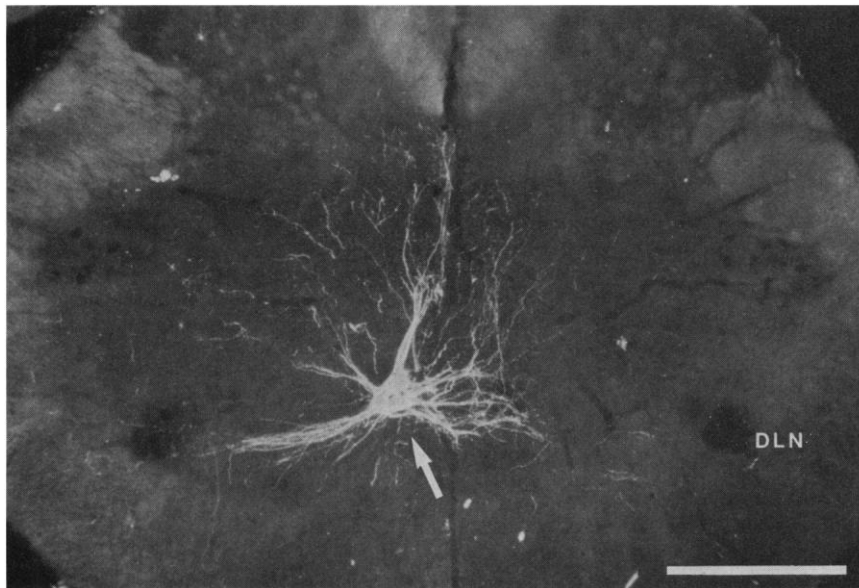
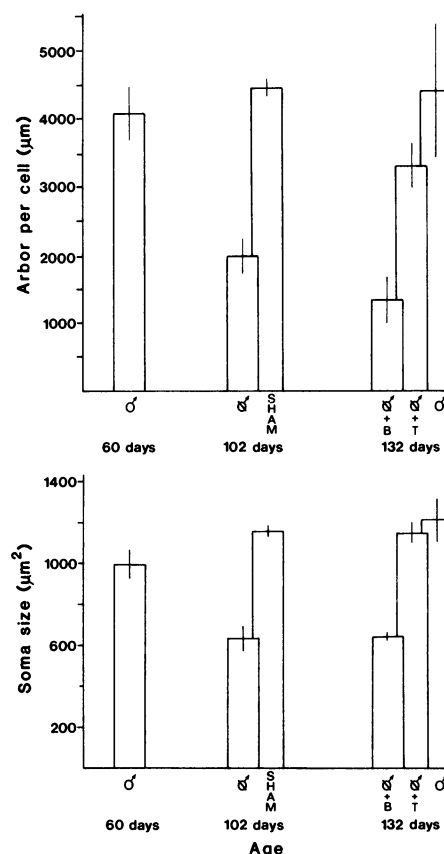


Fig. 1. Dark-field photomicrograph of a 40- $\mu\text{m}$  transverse section through the lumbar spinal cord of a normal adult male rat after injection of CT-HRP into the bulbocavernosus muscle. Arrow indicates four HRP-labeled SNB motoneurons; DLN, dorsolateral nucleus; calibration bar, 500  $\mu\text{m}$ .

castrated ( $n = 5$ ) at 60 days of age and then killed 6 weeks later at 102 days of age; an additional set of castrated rats that were implanted 6 weeks after surgery with Silastic tubes (13) that either contained testosterone ( $n = 5$ ) or were empty ( $n = 4$ ), and killed 4 weeks later at 132 days of age; a final set of normal males 132 days old ( $n = 2$ ).

Because it was necessary to examine the dendritic arbor of directly comparable sets of motoneurons in all groups and because of the heterogeneity of SNB motoneuron projections in males, we used cholera toxin conjugated to horseradish peroxidase (CT-HRP, List Biological) to label retrogradely only those SNB motoneurons projecting to the sexually dimorphic BC. This method produces extensive dendritic labeling and, in some cases, is more sensitive than Golgi staining (14). We used CT-HRP to study dendritic morphology rather than the more traditional Golgi methods because (i) it allowed identification of motoneurons by their projections, and (ii) the capriciousness and small number of neurons stained by Golgi techniques (in conjunction with the small number of SNB motoneurons) would make the number of animals necessary to obtain a reliable result prohibitively large. To visualize SNB motoneurons and their processes we injected 0.5  $\mu\text{l}$  of a 0.2 percent solution of CT-HRP into the left BC. After 48 hours, a period shown in pilot studies to be optimal for maximal transport and visualization of HRP, all animals were deeply anesthetized with urethane and perfused intracardially first with saline and then with cold 1 percent paraformaldehyde and 1.25 percent glutaraldehyde. The lumbar portion

of the spinal cord was then removed, post-fixed briefly, and embedded in gelatin, and 40- $\mu\text{m}$  frozen sections were cut transversely. To minimize possible variability in the HRP reactions, which might produce differences in the degree of dendritic labeling across groups, spinal cords from several groups were embedded in the same gelatin block



and processed together. Sections were incubated with tetramethylbenzidine (15), and alternate series were counterstained with thionine or neutral red.

To estimate the length of SNB motoneuron processes, one series of sections (every fourth section, 160  $\mu\text{m}$  apart) through the SNB region was examined under dark-field illumination and all HRP-filled somas and processes were drawn at a final magnification of 180 $\times$  with a camera lucida. The length of each HRP-filled process was measured from these drawings with a digitizing tablet interfaced with a computer. The sum of these lengths for each animal was divided by the number of labeled motoneuron somas observed in that series to yield an estimate of the dendritic arbor per cell (16). Although this estimate may not represent the actual length of the dendritic arbor of an SNB motoneuron, the analysis does permit a comparison of overall dendritic length among groups of animals. In addition, all HRP-filled SNB somas were categorized visually under bright-field illumination as being lightly or heavily labeled. Finally, 8 to 12 HRP-labeled somas in each animal were drawn at a final magnification of 400 $\times$  and their cross-sectional areas were measured (17).

Injections of CT-HRP into the BC produced extensive labeling of SNB somas that were ipsilateral to the injection site and the processes of these cells (Fig. 1). The dendritic arbor of SNB motoneurons that project to the BC in normal adult males was quite large, having a lateral diameter of at least 2000  $\mu\text{m}$ . The arbor was distinctive, distributed bilaterally into the dorsolateral nuclei (DLN) and lateral funiculi, and dorsally through lamina X. Many dendrites from SNB motoneurons also project across the midline and are frequently closely apposed to contralateral SNB somas. The length of the dendritic arbor per labeled cell in normal and sham-castrated males was not different, ranging from 4070 to 4470  $\mu\text{m}$  [ $F(1, 19) = 0.41, P > 0.2$ ] (Fig. 2). However, 6 weeks after castration, the average dendritic length per motoneuron in castrated males was reduced to approximately 1970  $\mu\text{m}$ , a decrease of 56 percent relative to that of sham-castrated males [ $F(1, 19) = 36.57, P < 0.0001$ ]. This decrease in dendritic length in castrated males could be reversed, and after 4 weeks of testosterone treatment dendritic arbor per cell was restored to

Fig. 2. Arbor per cell (top) and soma size (bottom) for normal males ( $\delta$ ), castrates ( $\delta$ ), sham-castrates, castrates with testosterone implants ( $\delta + T$ ), and castrates with blank implants ( $\delta + B$ ). Bar height represents average values  $\pm$  SEM,  $n = 4$  to 5 per group except for normal males at 132 days where  $n = 2$ .

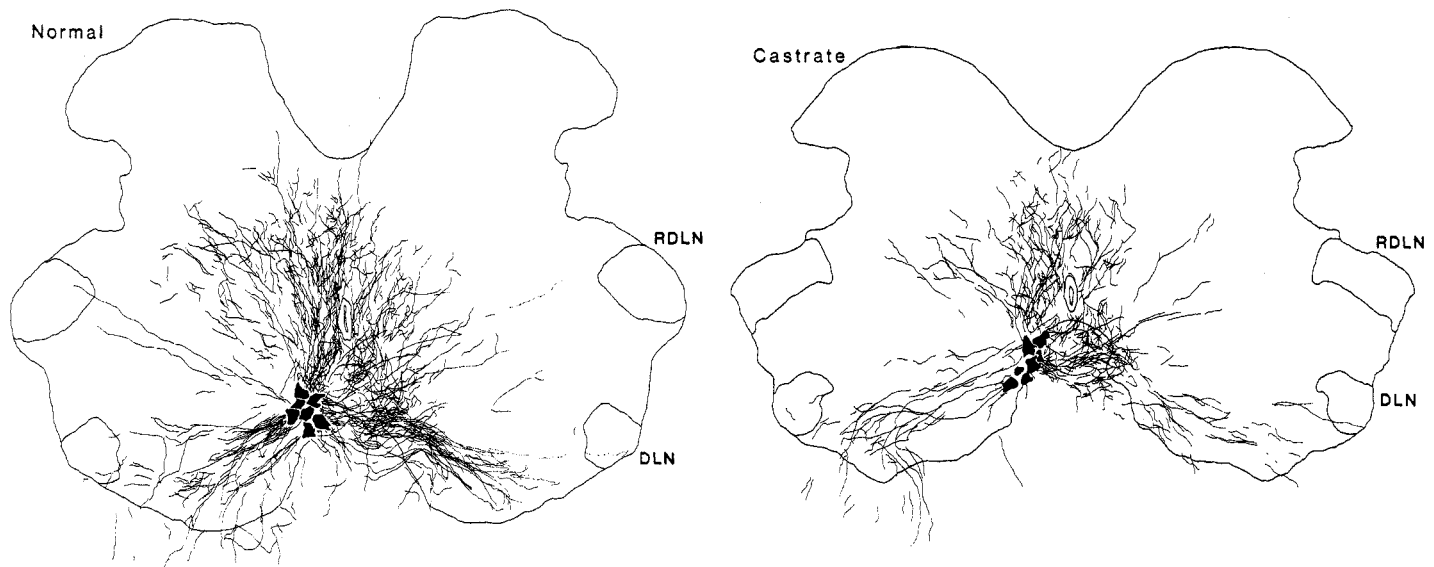


Fig. 3. Camera lucida composites of HRP-labeled processes drawn at 320  $\mu\text{m}$  intervals over the total extent of the SNB of a normal male (left) and a castrated male (right). The animals represented were chosen for maximal comparability; the number of labeled motoneurons, density of labeling, and rostral-caudal length of the SNB do not differ. Although overall dendritic

length is reduced in castrated males, processes extending to the dorsal and lateral funiculi can be observed in both cases. Motoneuronal somas (filled-in) are shown to indicate the location of the SNB; DLN, dorsolateral nucleus; RDLN, retrodorsolateral nucleus; calibration bar, 500  $\mu\text{m}$ .

normal levels [ $F(1, 19) = 4.07, P > 0.05$ ]. The arbor per cell of castrated males with blank implants remained significantly lower than that of testosterone-treated or normal males [ $F(1, 19) > 10.0, P < 0.005$ ], but did not differ from that of unimplanted castrated males [ $F(1, 19) = 2.21, P > 0.15$ ]. The pattern of changes observed in the SNB soma area was identical, replicating the finding of Breedlove and Arnold (9). Soma area was reduced by 45 percent in castrated males compared to sham-castrates [ $F(1, 19) = 54.60, P < 0.0001$ ]. Four weeks of testosterone treatment restored soma size to normal levels [ $F(1, 19) = 0.38, P > 0.5$ ]. Average SNB soma area in castrated males with blank implants was significantly lower than that of normal males or castrates with testosterone implants [ $F(1, 19) > 45.60, P < 0.0001$ ] but did not differ from that of unimplanted castrates [ $F(1, 19) = 0.03, P > 0.8$ ].

It is possible that HRP transport efficiency was diminished by the androgen depletion in castrates, resulting in artifactually smaller dendritic lengths. However, several lines of evidence make this possibility unlikely. (i) The number of SNB motoneurons filled by our HRP injections was the same among groups [ $F(5, 19) = 1.61, P > 0.2$ ]. Thus, differences in the amount of labeled dendritic arbor could not be attributed to differences in the overall number of labeled motoneurons [an average of  $48.5 \pm 2.53$  (SEM), corrected by the method of Abercrombie (18)]. Moreover, any differences in the number of labeled somas observed were taken into account by dividing the total

dendritic length per animal by the number of labeled motoneurons. (ii) The average number of heavily labeled SNB motoneuron somas per animal did not differ between groups [ $F(5, 19) = 1.53, P > 0.2$ ]; an average of  $79.7 \pm 2.31$  (SEM) percent of HRP-filled somas fell in this category. This result suggested that HRP transport to the soma was unaffected by castration or hormonal treatment. (iii) The maximal distance from the SNB at which labeled processes could be observed was identical in all groups. For example, the fact that processes extended well into the dorsal and lateral funiculi in all animals indicated that HRP was transported to the same degree in these dendrites in all groups (Fig. 3). (iv) It seems unlikely that such a substantial decrease (56 percent) in dendritic length could be accounted for by transport deficiency alone.

Changes in dendritic morphology can have profound consequences for synaptic connectivity and neuronal function. For example, dendritic geometry may affect a neuron's electrical properties or modulate the number or organization of synaptic inputs (19). Furthermore, recent evidence for an ongoing extension and retraction of dendritic processes (20) suggests that there is a dynamic, structural regulation of neuronal function. Our results indicate that androgens can be involved in this process by regulating the length of dendrites and the size of motoneuronal somas in adulthood. Decreased circulating androgen causes a reduction in dendritic length that is increased again with increased androgen. This type of androgen-dependent, reversible anatomical

plasticity has not been previously demonstrated in an adult mammalian system. This finding is particularly exciting because changes in androgen levels occur normally in the life of the male rat [for example, at puberty or senescence (21)] and correlate with changes in the frequency of copulatory behaviors (5). Thus, such fluctuations in androgen levels may alter the morphology and functioning of androgen-sensitive neurons. For example, the dramatic decrease in SNB dendritic length and soma size observed after castration may represent a decrease in the membrane area available for synaptic contacts, a decline in the number of synapses, or changes in physiological characteristics of the SNB motoneurons. Such changes, whether produced experimentally or through normal fluctuations in androgen titers, may therefore be associated with alterations in the connectivity and physiology of SNB motoneurons and in their ultimate function in copulatory behavior.

#### REFERENCES AND NOTES

1. A. P. Arnold and R. A. Gorski, *Annu. Rev. Neurosci.* 7, 413 (1984); L. Plapinger and B. S. McEwen, in *Biological Determinants of Sexual Behavior*, J. B. Hutchinson, Ed. (Wiley, New York, 1978), pp. 153–218.
2. A. P. Arnold and S. M. Breedlove, *Horm. Behav.* 19, 469 (1985).
3. T. J. DeVogd and F. Nottebohm, *Science* 214, 202 (1981); T. J. DeVogd, B. Nixdorf, F. Nottebohm, *Brain Res.* 329, 304 (1985).
4. B. L. Hart and P. Y. Melese-D'Hospital, *Physiol. Behav.* 31, 802 (1983).
5. K. Larsson, in *Endocrine Control of Sexual Behavior*, C. Beyer, Ed. (Raven, New York, 1979), pp. 77–163; B. L. Hart, in *Sex and Behavior*, T. E. McGill, D. A. Dewsbury, B. D. Sachs, Eds. (Plenum, New York, 1978), pp. 205–242.

6. S. M. Breedlove and A. P. Arnold, *Science* **210**, 564 (1980); H. D. Schroder, *J. Comp. Neurol.* **192**, 567 (1980).
7. R. Cihak, E. Gutmann, V. Hanzlikova, *J. Anat.* **106**, 93 (1970).
8. K. E. McKenna and I. Nadelhaft, *Soc. Neurosci. Abstr.* **10**, 902 (1984).
9. S. M. Breedlove and A. P. Arnold, *Brain Res.* **225**, 297 (1981).
10. E. J. Nordeen, K. W. Nordeen, D. R. Sengelaub, A. P. Arnold, *Science* **229**, 671 (1985); S. M. Breedlove and A. P. Arnold, *J. Neurosci.* **3**, 417 (1983); *ibid.*, p. 424; D. R. Sengelaub and A. P. Arnold, *ibid.*, in press.
11. S. M. Breedlove and A. P. Arnold, *J. Comp. Neurol.* **215**, 211 (1983); J. Y. Dube, R. Lesage, R. R. Tremblay, *Can. J. Biochem.* **54**, 50 (1976).
12. P. Wainman and G. C. Shipounoff, *Endocrinology* **29**, 955 (1941); S. Tucek, D. Kostirova, E. Gutmann, *J. Neurol. Sci.* **27**, 353 (1976).
13. 3.18 mm outer diameter; 1.57 mm inner diameter; 45 mm long; length of tubing was calculated to give plasma titers of androgen in the high physiological range [E. R. Smith, D. A. Damassa, J. M. Davidson, in *Methods in Psychobiology*, R. D. Meyer, Ed. (Academic Press, New York, 1978), vol. 3, pp. 259-279].
14. X. S. T. Wan, J. Q. Trojanowski, J. O. Gonatas, C. N. Liu, *Exp. Neurol.* **78**, 167 (1982); E. M. Kurz, D. R. Sengelaub, A. P. Arnold, *Soc. Neurosci. Abstr.* **11**, 529 (1985).
15. M. M. Mesulam, *J. Histochem. Cytochem.* **27**, 106 (1978).
16. Uncorrected numbers of labeled motoneurons yield a conservative estimate of group differences in arbor per cell. If corrections for cell size were made, the difference in arbor per cell between the high- and low-androgen groups would be artifactually accentuated [due to the larger soma size in the high-androgen group (18)].
17. Two additional measures were taken to gauge the comparability of the spinal cords among groups. For each cord, the outline of the gray matter in every section examined was traced using a microprojector and the average gray matter area calculated; the rostral-caudal length of the SNB was also determined in each animal. No differences were observed in either measure [ $F(5, 19) < 1.6, P > 0.2$ ], indicating that cords did not shrink after castration or show overall growth due to androgen treatment.
18. B. W. Konigsmark, in *Contemporary Research Methods in Neuroanatomy*, W. S. H. Nauta and S. O. E. Ebbesson, Eds. (Springer-Verlag, New York, 1970), pp. 315-340.
19. D. Purves and J. W. Lichtman, *Science* **228**, 298 (1985).
20. R. D. Hadley and D. Purves, *Soc. Neurosci. Abstr.* **11**, 963 (1985).
21. C. Corpechot, E.-E. Baulieu, P. Robel, *Acta Endocrinol.* **96**, 127 (1981); R. Ghanadian, J. G. Lewis, G. D. Chisholm, *Steroids* **25**, 753 (1975); M. T. Peng *et al.*, *Gerontology* **29**, 32 (1983).
22. We thank S. W. Bortjer and E. A. Brenowitz for their comments on the manuscript. This work was supported by USPHS HD15021 to A.P.A. and NRSA NS07355-02 to D.R.S.

18 November 1985; accepted 7 February 1986

## Amplification and Rearrangement of *Hu-ets-1* in Leukemia and Lymphoma with Involvement of 11q23

UGO ROVIGATTI,\* DENNIS K. WATSON, JORGE J. YUNIS

The *Hu-ets-1* oncogene was found to be rearranged and amplified 30-fold in one case of acute myelomonocytic leukemia in which a homogeneously staining region occurred on 11q23; the oncogene was rearranged and amplified approximately tenfold in a case of small lymphocytic cell lymphoma with an inverted insertion that also involved band 11q23. This work suggests that *Hu-ets-1* is an unusual oncogene that can help explain the common involvement of chromosome band 11q23 in various subtypes of hematopoietic malignancies.

THE PRESENCE OF *ETS* AND *MYB* IN the acute leukemia virus E26 produces at least two differences in the pathogenicity of this virus as compared to the myeloblastosis virus AMV, which contains only *myb*: (i) leukemias with a myeloid as well as an erythroid phenotype are induced in birds infected by E26 and (ii) myeloblasts transformed by E26 appear to be completely blocked in differentiation and are not inducible by tumor promoters (1). While two different *c-ets* loci have been detected in the human, mouse, and cat genomes (2), a single colinear *c-ets* homologue may be present in the chicken genome. In humans, these loci were called *Hu-ets-1* and *Hu-ets-2* (2) and were mapped to chromosome bands 11q23-24 (3) and 21q22.3, respectively (2). Specific chromosomal abnormalities involving 11q23—such as reciprocal translocations, deletions, in-

verted insertions (*inv ins*), and homogeneously staining regions (HSR's) (4-6)—have been associated with acute myelomonocytic leukemia (AMMoL) (4), acute

lymphocytic leukemia (ALL) and small lymphocytic cell lymphoma (SLCL) (5), and myeloproliferative syndromes (6). Because of these observations, we decided to investigate whether *Hu-ets-1* is altered in leukemic and lymphomatous cells with 11q23 chromosomal abnormalities.

The G-banding pattern on chromosome 11 from patient 1 with AMMoL (M4) and an HSR 11q23 as the only chromosomal defect is shown in Fig. 1A; Fig. 1B displays an *inv ins*(21;11)(q22.3; q23q14.2), +21 in an SLCL patient (patient 2). In patient 2, the segment 11q14.2q23 from one chromosome 11 is inverted before being inserted into band 21q22 so that band 11q23 [where *Hu-ets-1* maps (2)] and band 21q22 [where *Hu-ets-2* maps (2)] become contiguous in the abnormally long chromosome 21.

The *Hu-ets-1* probe, pRD6K (Fig. 2A), is a 5.7-kilobase (kb) fragment of human DNA (2). Southern blot hybridization (7) revealed amplification of *Hu-ets-1* in Bam HI-digested DNA from patients 1 and 2 (Fig. 2B). For comparison, a normal blood donor DNA sample obtained during chemotherapy-induced remission from patients 1 and 2 are shown.

In the case of the DNA from patient 1, an additional band of approximately 9.0 kb was present after Bam HI digestion. The signal intensity from the rearranged fragment was slightly less than the high signal intensity of the other amplified band which migrated with the same mobility as the 14-kb band present in normal controls.

Additional evidence for the amplification as well as rearrangement of *Hu-ets-1* was obtained by digesting DNA from patients 1 and 2 with the restriction enzyme Xba I and by hybridizing the blots with the pRD6K probe. Both patients showed evidence of amplification and rearrangement (Fig. 2C, lanes 4 and 5).

Rearrangement was indicated by the pres-

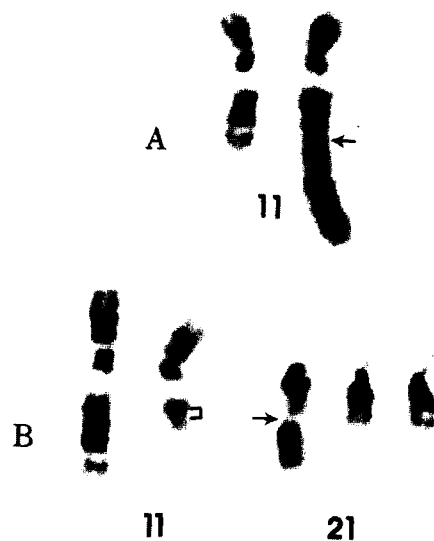


Fig. 1. Pairs of G-banded chromosomes 11 in patient 1 with acute myelomonocytic leukemia (AMMoL) and an HSR 11q23 (A); and chromosomes 11 and 21 in patient 2 with small lymphocytic cell lymphoma (SLCL) with *inv ins*(21;11)(q22.3; q23q14.2), +21 (B).

U. Rovigatti, Laboratory of Human Neoplasia, A. Ochsner Medical Foundation, New Orleans, LA 70121. D. K. Watson, Laboratory of Molecular Oncology, National Cancer Institute, Frederick, MD 21701. J. J. Yunis, Department of Laboratory Medicine and Pathology, University of Minnesota Medical School, Minneapolis, MN 55455.

\*To whom correspondence should be addressed.